A Virtual Excavation: Combining 3D Immersive Virtual Reality and Geophysical Surveying

Albert Yu-Min Lin∗, Alexandre Novo†, Philip P. Weber∗, Gianfranco Morelli†, Dean Goodman‡, Jürgen P. Schulze∗

∗California Institute for Telecommunications and Information Technology, University of California San Diego, La Jolla, CA, 92093, USA

†Geostudi Astier, via A. Nicolodi, 48 Livorno 57121, Italy

‡Geophysical Archaeometry Laboratory, 20014 Gypsy Ln, Woodland Hills, CA 91364, USA

Abstract. The projection of multi-layered remote sensing and geophysical survey data into a 3D immersive virtual reality environment for non-invasive archaeological exploration is described. Topography, ultra-high resolution satellite imagery, magnetic, electromagnetic, and ground penetrating radar surveys of an archaeological site are visualized as a single data set within the six-sided (including floor) virtual reality (VR) room known as the StarCAVE. These independent data sets are combined in 3D space through their geospatial orientation to facilitate the detection of physical anomalies from signatures observed across various forms of surface and subsurface surveys. The data types are highly variant in nature and scale, ranging from 2D imagery to massive scale point clouds. As a reference base-layer a site elevation map was produced and used as to normalize and correlate the various forms of collected data within a single volume. Projecting this volume within the StarCAVE facilitates immersive and collaborative exploration of the virtual site at actual scale of the physical site.

1 Introduction

Non-invasive investigations of subsurface anomalies through geophysical surveys can provide archaeologists with valuable information prior to, or in-place of, the non-reversible processes of excavation. This can be extremely useful, especially in cases where excavation is not an option or restricted. Furthermore, these tools can be used to monitor the state of preservation of sites or monuments through nondestructive analysis [1].

Geophysical methods, such as magnetic [2, 3], electromagnetic (EM) [4–6], and ground penetrating radar (GPR) [7, 8], detect features by observing variations of physical properties of materials within a matrix. Each of these methods exploits different physical properties to generate maps of the variations. Magnetic survey is a passive detection of contrasts in the magnetic properties of differing

materials, whereas EM surveys measure the conductivity and magnetic susceptibility of soil by inducing eddy currents through a generated electromagnetic field. GPR transmits an electromagnetic pulse and measures a reflected signal that is dependent upon the dielectric properties of subsurface material [9]. With GPR, it is possible to reconstruct high-resolution 3D data visualizations of the composition of the subsurface [10–12].

While there have been many impressive advances in data processing techniques to enable this, less focus has been applied to the potential of non-standard visualization environments to further the ability to generate virtual representation of the subsurface. For example, the "StarCAVE" is a virtual reality (VR) environment operating at a combined resolution of 68 million pixels, 34 million pixels per eye, distributed over 15 rear-projected wall screens and 2 down-projected floor screens [13]. The goal of this paper is to explore the use of the StarCAVE to enable non-invasive "virtual excavation" through the 3D VR reconstruction of geophysical survey data of an archaeological site that was investigated in July, 2010 as a component of the Valley of the Khans Project, a non-invasive remote sensing survey for burial sites in Northern Mongolia. Due to local customs that prohibit the destruction of any burial grounds, this case study serves as an example where geophysics and virtual reality representations of archaeological sites provide an alternative to destructive surveys.

The rest of the paper is organized as follows. First we look at related work. In Section 3, we describe the data collection, processing and visualization methods used in this study. In Section 5, we discuss our results and observations of 3D virtual reality visualization of the data. Finally, Section 6 summarizes our main conclusions.

2 Related Work

There are not many fully featured software tools for the visualization of ground penetrating radar data sets. One example is AEGIS Easy 3D [14]. None of them, however, supports immersive 3D environments, and can thus not take advantage of the high resolution and to scale capabilities of CAVE-like systems.

Some prior work uses direct volume rendering for the display of the data [15–19], which would require resampling our data since the GPR data needs to be displayed in a way that follows the shape of the terrain. Billen et al. [20] created an immersive application for CAVE environments, but it does not allow visualizing the data as points, which permit very precise analysis of the data on the basis of individual data values and allow for the data to follow the terrain it is under.

3 Data Collection Methods

A 85 x 80 meter archaeological site was identified for survey by observing surface artifacts in and around the roots of fallen trees. A site grid comprised of 5 x 5 meter cells oriented along the geographical north was marked in the field in order

to acquire data in a regular pattern as neither GPS nor Total station was used. Each grid was positioned based on local coordinates and data were collected following parallel lines spaced by 25 cm. Sub-meter resolution GPS was used to record the UTM coordinates of the corners of the grid.

An Overhouser gradiometer was used in this study. During the survey, the distance between sensors was set at 1.5m and the distance between the lower of the two sensors and the ground was maintained at 0.2m. Data was collected in "fast walking" mode at 0.5 seconds cycling rate following parallel North-South transects approximately 1m apart. The internal sub-meter GPS of the gradiometer was employed for data positioning.

The EM-38 electromagnetometer creates measurements of ground conductivity (quad-phase) in milliSiemens per meter (mS/m) and magnetic susceptibility (in-phase) in parts per million. The maximum effective depth range (1.5 m) was achieved by collecting data in the vertical dipole mode. Data collection was performed in walking mode at a cycling rate of 2 readings per second following parallel transects approximately 1m apart. An internal sub-meter GPS recorded geospatial positions of scans and an external data logger allowed the operator to view position and raw data in real time.

Fig. 1. GPR survey of this study's field site in Northern Mongolia with the IDS dual frequency antenna detector.

This study used a IDS GPR system with a dual frequency antenna at 250 MHz and 700 MHz for simultaneous investigation of deep and shallow targets, respectively, as seen in Figure 3. Parallel profiles 0.25 meters apart were followed using string as a guideline, in order to assist the operator in pushing the GPR antenna across a generated surface grid [7]. This method, along with 3D visualization techniques, have been widely applied in GPR surveys for archaeology [21, 22].

Time slices represent maps of the amplitudes of the recorded reflections across the survey area at a specified time. The processed reflection traces in all reflection profiles were then used to generate three-dimensional horizontal slices by

spatially averaging the squared wave amplitudes of the recorded radar reflections over the time window. The interpolation process creates interpolated time-slices, which are normalized to 64 bits following the color changes between different levels and not actual reflection values. The number of slices depends on the length of the time window selected, the slice thickness and the overlay between slices. Thickness of horizontal slices is often set to at least one or two wavelengths of the radar pulse that is sent into the ground.

The raw data set size is 153MB. The resolution of the recorded data was preserved in the visualization. The radargrams were resampled to a constant number of scans per marker. We signed a marker about every meter, 32 new scans were made between meter markers. This step creates an equidistant scan distribution along the radargrams. The uneven terrain where data were collected produces slips of the survey wheel which affects constant scan distribution along the profiles.

3.1 Data Preprocessing

A digital model terrain (DMT) map of the grid was generated from measurements made at each cell corner to reference small changes in the topography of the site using the software Google SketchUp. Two-dimensional EM and MAG images were warped onto the surface topography map within Google SketchUp by matching georeferenced 2D geophysical data with the UTM coordinates of each grid corner.

Three-dimensional GPR sub-cubes of each sampling area were generated from processed radargrams. A complete 3D cube of the entire site was generated by merging the point clouds of each sub-cube. Finally, this cube is corrected for topography from the overlapping DMT model of the entire site. A diagram of the various data layers (with a single depth-slice representation of GPR data is seen in Figure 2.

To model the site and data correctly in a virtual environment, the terrain was first constructed and then the subsurface radar data was mapped to the terrain model. The terrain was created with the localized height data as a height field. The data consisted of a grid of 5×5 meter squares where at each corner a vertical difference in meters was collected relative to a local origin. The subsurface radar data that was collected consisted of a local position relative to the local origin, a depth and intensity value. The depth value that was collected was relative to the surface, therefore the data depth was preprocessed by bi-linear interpolating the values from the height field. This resulted in the visualized subsurface data correctly following the contours of the generated terrain model.

4 Software Implementation

The software application was written as a C++ plug-in for CalVR, see Figure 3. CalVR is a virtual reality middleware framework developed at UCSD for the purpose of providing a modern VR software environment which can drive any

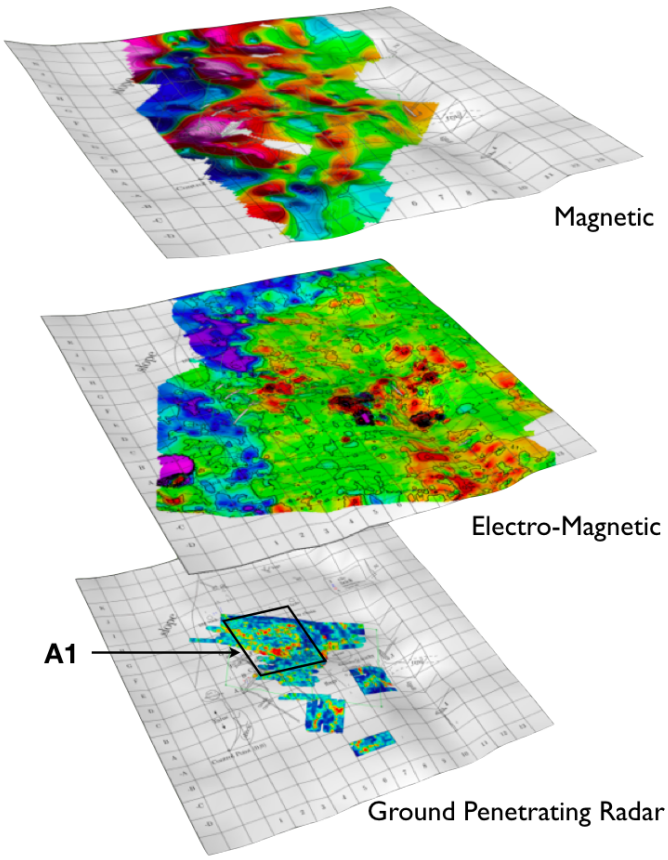

Fig. 2. Three layers of geophysical data warped over a topographical site map generated in Google SketchUP.

kind of VR display system, and use all typical tracking systems. CalVR is free and open source and was developed for the VR community as a research platform. Plug-ins are separately compiled dynamic libraries which integrate into CalVR in a modular fashion, i.e., they can be active or deactive in any given VR session. CalVR internally uses the OpenSceneGraph API [23] for its graphical objects. Most plug-ins create their visual elements in OpenSceneGraph (OSG) as well, but it is possible to use OpenGL directly, encapsulated in a simple OSG node so that OpenGL based graphics can co-exist with OSG-based graphics. The application at hand uses a combination of OpenGL and OSG-based graphical elements.

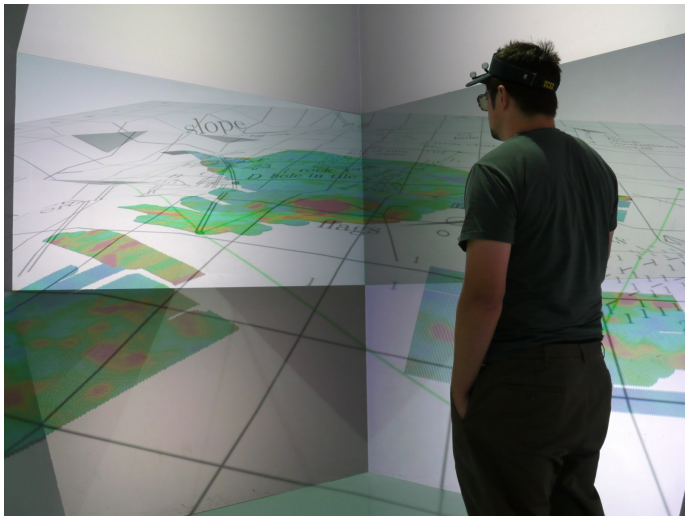

Fig. 3. Site topography map and GPR data displayed as a stereo projection within the StarCAVE virtual reality environment (images in paper show only one stereo channel).

4.1 Surface Textures

For spatial context, the user can select one of three different surface textures: it can either just be the 5×5 meter grid, which also contains some textual information and landmarks, or it can be the grid along with magnetic surface information, or it can be the grid with the electro-magnetic data set superimposed on it. Figure 4 illustrates these options. The user can switch through these three options but moving a little joystick on the VR wand up or down. OSG's Terrain class manages surface structure and textures. The coordinate system is such that +x is east, +y is north, and +z is depth from the surface. We render the surface texture translucent at an alpha level of 50% so that it cannot occlude the subsurface radar data. The surface textures are user configurable: additional textures can easily be added, and they can be in any image format OSG supports; we currently use PNG.

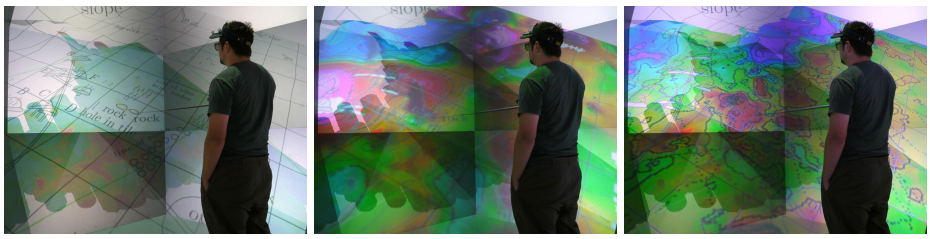

Fig. 4. Three map modes: just topology, magnetic, electro-magnetic.

4.2 Subsurface Radar Data

We display the subsurface radar data as a collection of points, see Figure 5. Each point represents a sample of the radar, which represents a volume of about one cubic centimeter. GPR values are available up to a depth of about 2-3 meters. The subsurface radar data set lists the points with x/y coordinates on the surface, but the z value is defined relative to the surface. Hence, in order to display the data in their correct positions in 3D, we calculate the height of the terrain at the respective x/y position and then offset the point by that amount. The x/y coordinates are on a regular grid, but not all grid cells actually contain data. This is why we store x/y coordinates with every point, rather than storing a list of heights with implicit x/y coordinates as an array. The points are spaced about a diameter apart, so that they create a continuous layer.

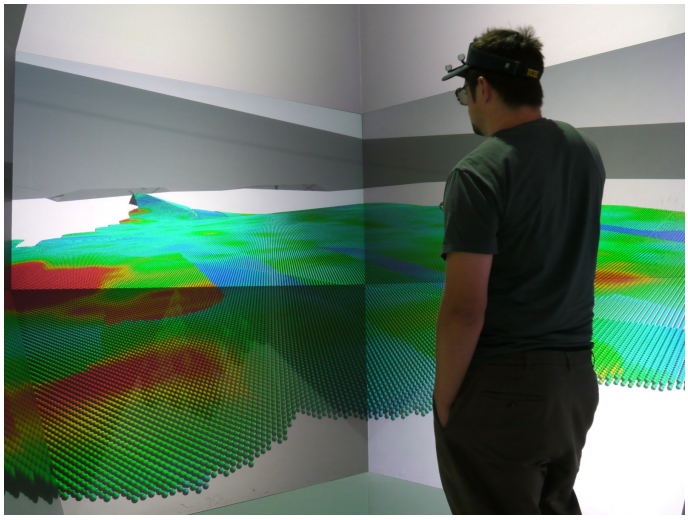

Fig. 5. Moving through GPR point cloud data in 3D virtual reality.

We color code the points based on density and use a color gradient from blue through green and yellow to red, to indicate different levels of density. The entire area of interest contains more than 13 million sample points. However, our rendering system is not capable of rendering this many points at once. Therefore, we only always render about one million points at once, in order to achieve an interactive rendering frame rate of about 30 frames per second in the StarCAVE. The samples are sorted by height, so that by rendering sets of one million points we display points of one or a maximum of two layers at a time. The user can switch between the point subsets by moving the little joystick on the wand left or right. Three different settings for height are shown in Figure 6. There is a short delay of less than a second whenever this switch happens, caused by the new set of points having to be loaded.

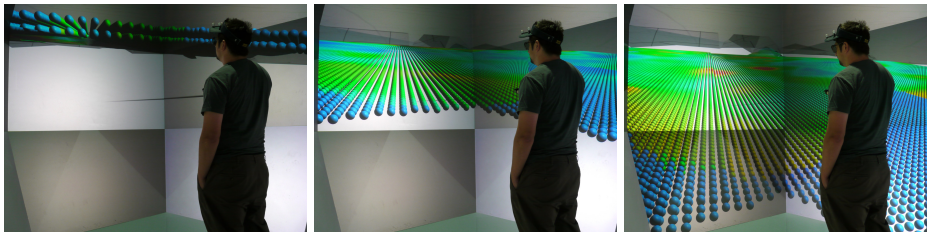

Fig. 6. Three different layers of GPR data.

Rendering one million points at interactive frame rates is not trivial. Plain OpenGL points always project to the same number of pixels on the screen, as opposed to an area which depends on how close the point is to the viewer. Therefore, we decided to use GLSL point sprites instead, which require the implementation of vertex and fragment shaders. We use the shaders from OSG's Compute example for CUDA programming [24]. This shader uses the OpenGL lighting parameters to achieve shading effects matching the shading of the rest of the scene. The transfer of the point data to the graphics card happens through a vertex buffer object (VBO). Whenever the user switches to another subset of points, this VBO gets filled with the new points. The colors for the points are determined by a pre-defined one-dimenstional, 256 element look-up table, which is pre-set with the aforementioned color gradient.

4.3 Usage Information

A complete data set for this application consists of the following files: a configuration file, one or more surface texture files, and one GPR sample data file. The configuration file contains information about the three texture files providing the ground textures, the grid size the textures are on (using 5x4 meter squares), the number of binary files referenced for the point data, and the names of those binary files. Each point in the binary file consists of 4 floats (x,y,z position and an intensity value). The points are sorted in x, y and z (height). At the end of the configuration file is a list of number triples for the height for select grid points, given as x/y and position within the 5x5 meter grid system. The OSGTerrain library will interpolate missing height data, so it is not critical that this list strictly follow the data grid.

Once the GPR plugin has been enabled in CalVR's configuration file, it can be run by passing the name of the configuration file to the executable: CalVR <config_file>.

5 Discussion

Representing the data at its original scale is one of the most important benefits of the visualization in virtual reality. Other benefits are that more data is visible

at a time thanks to the high pixel count in the StarCAVE. Another benefit of the application is that the switching through the various layers of GPR data happens almost immediately. This takes significantly longer with the desktop-based software the researchers use, presumably because the virtual reality application was specifically designed for GPR data display.

The choice of displaying the data as points showed to be good because this makes it easy to render the data just below the terrain, following the terrain surface. Since each point has its own position, it is easy to modify this position to always be a certain amount below the surface.

6 Conclusions

The representation of data in virtual reality space allows an immersive projection of data at its original scale. The reconstruction of geophysical data in virtual space is an especially relevant application of 3D visualization, where physical exploration is not possible and virtual exploration is limited by methods of collection and visualization. The presented software application for the StarCAVE allows quicker insight into the data than desktop based methods can, and it can show more data at a time.

References

1. Watters, M.S.: Gpr: a tool for archaeological management. In: Proceedings of the Tenth International Conference on Ground Penetrating Radar, 2004. GPR 2004. (2004) 811 – 815
2. Becker, H.: From nanotesla to picotesla-a new window for magnetic prospecting in archaeology. Archaeological Prospection **2** (1995) 217–228
3. Aitken, M.J.: Magnetic prospecting. i. the water newton survey. Archaeometry **1** (1958) 24–26
4. Frohlich, B., Lancaster, W.: Electromagnetic surveying in current middle eastern archaeology: Application and evaluation. Geophysics **51** (1986) 1414–1425
5. Tabbagh, A.: Applications and advantages of the slingram electromagnetic method for archaeological prospecting. Geophysics **51** (1986) 576–584
6. Abu Zeid, N., Balkov, E., Chemyakina, M., Manstein, A., Manstein, Y., Morelli, G., Santarato, G.: Multi-frequency electromagnetic sounding tool EMS. Archaeological discoveries. Case stories. EGS - AGU - EUG Joint Assembly, Nice, France **5** (2003)
7. Novo, A., Grasmueck, M., Viggiano, D., Lorenzo, H.: 3D GPR in archaeology: What can be gained from dense data acquisition and processing. In: Twelfth International Conference on Ground Penetrating Radar. (2008)
8. Goodman, D., Nishimura, Y., Rogers, J.: GPR time slices in archaeological prospection. Archaeological prospection **2** (1995) 85–89
9. Davis, J., Annan, A.: Ground penetrating radar for high-resolution mapping of soil and rock stratigraphy. Geophysical Prospecting **37** (1989) 531–551
10. Watters, M.S.: Geovisualization: an example from the catholme ceremonial complex. Archaeological Prospection **13** (2006) 282–290
11. Nuzzo, L., Leucci, G., Negri, S., Carrozzo, M., Quarta, T.: Application of 3d visualization techniques in the analysis of gpr data for archaeology. Annals Of Geophysics **45** (2009) 321–337

12. Grasmueck, M., Weger, R., Horstmeyer, H.: Full-resolution 3d gpr imaging. Geophysics **70** (2005) K12–19
13. DeFanti, T.A., Dawe, G., Sandin, D.J., Schulze, J.P., Otto, P., Girado, J., Kuester, F., Smarr, L., Rao, R.: The starcave, a third-generation cave and virtual reality optiportal. Future Generation Computer Systems **25** (2009) 169 – 178
14. Instruments, A.: Easy 3D - GPR Visualization Software. URL: http://www.aegis-instruments.com/products/brochures/easy-3d-gpr.html (2010)
15. Ropinski, T., Steinicke, F., Hinrichs, K.: Visual exploration of seismic volume datasets. Journal Proceedings of the 14th International Conference in Central Europe on Computer Graphics, Visualization and Computer Vision (WSCG06) 14 (2006)
16. Chopra, P., Meyer, J., Fernandez, A.: Immersive volume visualization of seismic simulations: A case study of techniques invented and lessons learned. IEEE Visualization (2002)
17. Winkler, C., Bosquet, F., Cavin, X., Paul, J.: Design and implementation of an immersive geoscience toolkit. IEEE Visualization (1999)
18. Froehlich, B., Barrass, S., Zehner, B., Plate, J., Goebel, M.: Exploring geo-scientific data in virtual environments. Proceedings of the conference on Visualization99, IEEE Computer Society Press (1999)
19. LaFayette, C., Parke, F., Pierce, C., Nakamura, T., Simpson, L.: Atta texana leafcutting ant colony: a view underground. ACM SIGGRAPH 2008 talks, ACM (2008)
20. (Billen, M., Kreylos, O., Hamann, B., Jadamec, M., Kellogg, L., Staadt, O., D. Sumner title=A geoscience perspective on immersive 3d gridded data visualization, publisher=Computers & Geosciences 34, y.p.)
21. Leckebusch, J.: Ground-penetrating radar: a modern three-dimensional prospection method. Archaeological Prospection **10** (2003) 213–240
22. Linford, N.: From hypocaust to hyperbola: ground-penetrating radar surveys over mainly Roman remains in the UK. Archaeological Prospection **11** (2004) 237 – 246
23. OpenSceneGraph: Scenegraph based graphics library. URL: http://www.openscenegraph.org (2004)
24. Orthmann, J., Keller, M., Kolb, A.: Integrating GPGPU Functionality into Scene Graphs. Vision Modeling Visualization (2009)